EUROPEAN ORGANIZATION FOR PARTICLE PHYSICS

LHCb-VELO 2000-98
20 October 2000

Measurements of the Signal Shape of a Silicon Strip Detector with SCTA Readout

Paolo Bartalini[1], Jan Buytaert[2], Paula Collins[2], Hans Dijkstra[2], Olivier Dormond[1], Markus Elsing[2], Frank Fiedler[2], Raymond Frei[1], Tjeerd Ketel[3], Sander Klous[3], Chris Parkes[1, now at 4], Thomas Ruf[2], David Steele[1], Leonard Studer[1], Frederic Teubert[2], and Victoria Wright[4]

[1] Insitut de Physique des Hautes Energies, Université de Lausanne, Bâtiment des Sciences Physiques, Dorigny, CH-1015 Lausanne
[2] European Laboratory for Particle Physics (CERN), Route de Meyrin 385, CH-1211 Genève
[3] Vrije Universiteit (VU), De Boelelaan 1079, NL-1007 MC Amsterdam
[4] University of Liverpool, Chadwick Building, Peach Street, Liverpool L69 7ZF, GB

Abstract

Data of a beam test in Autumn 1999 have been analysed to determine the pulse shape of the signal as read out by an SCTA chip from a detector prototype for the LHCb Vertex Locator. The measurements have been performed at different bias voltages and distinguishing non-irradiated and irradiated regions on the detector. The results are interpreted in terms of the signal overspill that remains for the subsequent readout after 25 ns, and an optimal working point is determined, considering both the signal amplitude and the overspill fraction.

1 Introduction

With bunch crossings at the LHC occuring at a rate of 40 MHz, fast readout of the detectors is mandatory to ensure that the signals from subsequent bunch crossings do not affect each other. One of the possible readout chips for the LHCb silicon strip vertex detector (Vertex Locator, "VELO") is the SCTA chip [1]. A non-irradiated and an irradiated region of a VELO prototype detector were each bonded to an SCTA readout chip, and their performance was tested during a beam test in Autumn 1999.

In this note, data from this beam test is analysed to determine the pulse shape obtained from the SCTA chips. In this context, the qualification of the SCTA chips for the LHCb VELO readout is verified. The signal fraction that remains 25 ns after the readout time is computed, and the optimal working point is determined.

Section 2 gives a description of the response of the SCTA chip to the charge signal from the silicon detector. In section 3, the test beam setup is briefly described. The analysis technique is discussed in some detail in section 4. In section 5, the results are presented and discussed. Some conclusions are drawn in section 6.

2 Description of the Response of the SCTA Chip

The charge signal as seen by the SCTA chip is parameterised in the following as a flat pulse, as shown schematically in figure 1. The relevant parameters are the rise time t_{rise}, width of the plateau t_{plateau}, and fall time t_{fall}. It should be noted that although this is only a crude approximation, this parameterisation describes the observed SCTA output well and is entirely sufficient for the purposes of this analysis. The Laplace transform is given by

$$F_{\text{pulse}}(s) = \frac{1}{s^2}\left(1 - e^{-t_{\text{rise}}s} - e^{-(t_{\text{rise}} + t_{\text{plateau}})s} - e^{-(t_{\text{rise}} + t_{\text{plateau}} + t_{\text{fall}})s}\right) . \tag{1}$$

The readout circuit can be parameterised to a good approximation by two double poles, giving rise to a bipolar output pulse shape [2]. Thus, the Laplace transfer function is given by

$$F_{\text{transfer}}(s) = \frac{s^2}{(s+a)^2\,(s+b)^2} , \tag{2}$$

where a and b denote the frequencies corresponding to the two poles.

The Laplace output response is then obtained as the product

$$F_{\text{output}} = F_{\text{pulse}}\,F_{\text{transfer}} . \tag{3}$$

The inverse of this function gives the time domain response $o(t)$: When defining

$$k(t) := \left(\frac{2}{(a-b)^3}\,e^{-at} + \frac{1}{(a-b)^2}\,t\,e^{-at} + \frac{2}{(b-a)^3}\,e^{-bt} + \frac{1}{(b-a)^2}\,t\,e^{-bt}\right) H(t) , \tag{4}$$

where the parameters a and b are defined above and $H(t)$ denotes a unit step function, one obtains

$$o(t) = k(t) - k(t - t_{\text{rise}}) - k\left(t - [t_{\text{rise}} + t_{\text{plateau}}]\right) + k\left(t - [t_{\text{rise}} + t_{\text{plateau}} + t_{\text{fall}}]\right) . \tag{5}$$

The shape of the time domain response $o(t)$ corresponding to the charge signal in figure 1 is shown in figure 2.

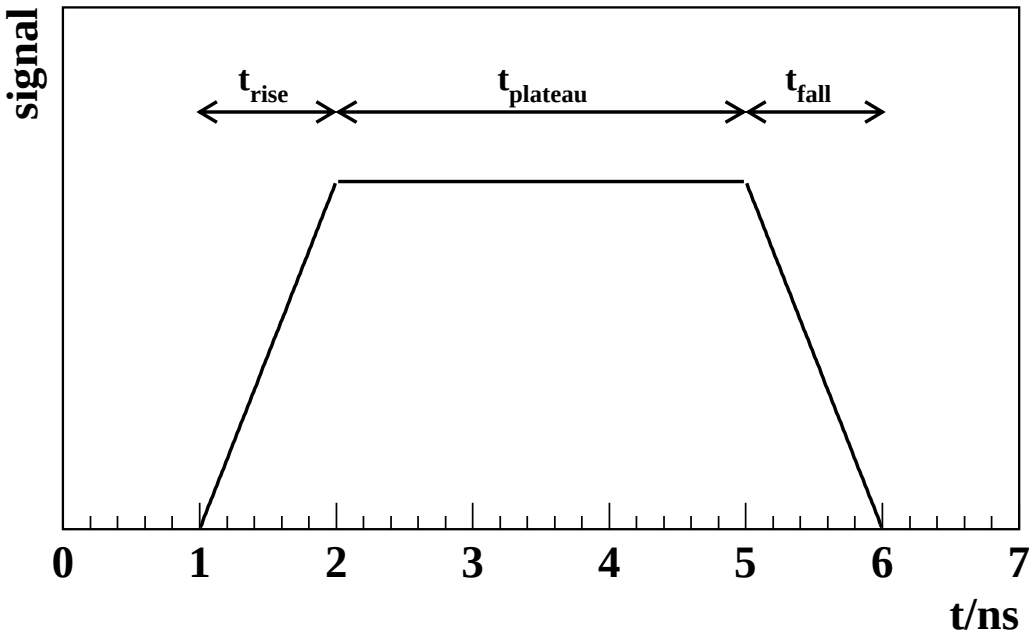

Figure 1: The parameterisation of the charge signal from the silicon detector as seen by the SCTA readout chip. A typical expected shape is shown. The scale of the vertical axis is arbitrary.

3 Test Beam Setup

A beam of 120 GeV pions from the CERN SPS traversed first the VELO prototype detector with SCTA readout, and also a DELPHI silicon detector which is not considered in this analysis. The SCTA detector is a 300 μm thick silicon detector with n strips on n bulk and strip pitches of 40 μm and 60 μm as described in [3]. It had two SCTA chips bonded to its concentric strips ("r" detector), where one chip read out the non-irradiated region of the detector and one the irradiated region, respectively. The signal pulse height was stored in an analog pipeline on the SCTA chips every 25 ns to simulate LHCb conditions. The clock speed for readout was 5 MHz.

Behind these detectors, a beam telescope was mounted. This consisted of three r and three ϕ VELO prototype detectors, each read out with VA2 chips. The position information in the plane of the SCTA detector needed for the analysis presented here is obtained from reconstructed tracks in the beam telescope.

Two scintillators were used to generate timing signals from the particles crossing the beam test setup. Events were stored if they were recorded within a window around the time signal provided by the scintillators. The timing precision of the scintillators was of the order of 1 ns which is sufficient not to introduce any bias in the pulse shape measurement.

4 Data Analysis

4.1 Analysis Strategy

In order to verify the description of the pulse shape and to determine the relevant parameters, it is necessary to measure the signal over a range of times. As can be seen from figure 2, the

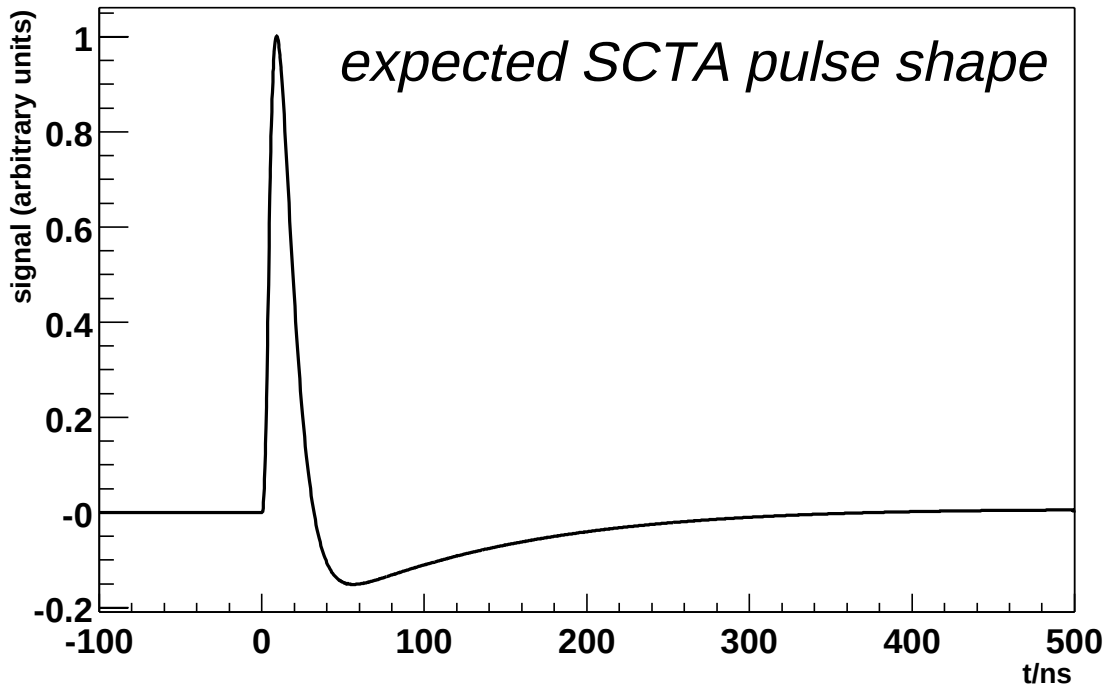

Figure 2: The expected time domain response of the SCTA readout chip to the input signal shown in figure 1 (corresponding to parameters $t_{\text{rise}} = 1\,\text{ns}$, $t_{\text{plateau}} = 5\,\text{ns}$, and $t_{\text{fall}} = 1\,\text{ns}$). The poles of the SCTA circuit have been set to $a = 1/7\,\text{GHz}$ and $b = 1/180\,\text{GHz}$.

expected signal goes through 0 after a relatively short time and produces an undershoot which is much shallower than the primary signal peak itself. Consequently, it is not sufficient for this analysis to rely on a clustering algorithm running on the charge information from the SCTA detector alone, because such an algorithm would not be able to distinguish "signals" of zero or very small amplitude from noise. On the other hand, summing up the charge on all detector strips would drown the signal in the large noise from strips that are far from the point where a particle passed the detector.

The strategy adopted in this analysis is to first reconstruct tracks in the beam telescope. These tracks are then extrapolated to the SCTA detector to obtain an expected hit point. Finally, the charge signal in a region around this expected point is summed.

The analysis program is embedded in the `VELOROOT` framework, which is described in detail in [4]. The data used for the analysis is summarized in table 1.

4.2 Alignment of the SCTA Detector

For the above technique to work, the SCTA detector has to be aligned with respect to the beam telescope, and the number of strips to be summed is dictated by the precision of this alignment.

The beam telescope has been aligned for previous analyses of the test beam data with the method described in [5]. For the alignment of the SCTA detector, clusters are formed from the charge information on the SCTA detector. A cluster is associated with a track in the telescope

bias voltage	runs	number of tracks
100 V	$558-565$ $568-570$ $575-577$ $579-590$	1642
150 V	$440-445$ $461-464$ $466+467$ $546-552$	743
200 V	$512-516$ $521-523$ $526-536$ $538-544$ $591-606$	4562

Table 1: A summary of the data used in the analysis. Runs for which timing information is not available (see section 4.3) are excluded from the table. Also not listed are runs 518, 525, 537, 545, 557, 566, and 567 which are very noisy (see section 4.6). The number of tracks with hits in all telescope stations passing fiducial cuts is also given. Each track corresponds to a measurement point in the histograms shown in figure 9.

if it passes the following requirements:

- The cluster is found within 12 ns of the signal peak. This ensures that only the best-measured clusters are used for the alignment.
- The distance between the weighted position of the cluster and the extrapolated track position is smaller than 1 mm.

The χ^2 resulting from the residuals between track and cluster positions is then minimized to obtain the alignment parameters.

Given the spacing along the beam axis of the SCTA detector and the telescope, the width of the distribution of residuals on the SCTA detector[1] is expected to be 5 times the position resolution of a single telescope r detector. The test beam setup has been moved twice during the experiment, and consequently the data cannot fully be described by one set of alignment parameters. Two sets of alignment parameters are however sufficient. The distributions of residuals are shown in figure 3. The widths of around 60 μm are within the expectation from the resolution of the telescope detectors.

For a detector with concentric strips, the alignment parameter describing the rotation angle about the axis perpendicular to the detector plane and passing through the center of the circular strips (alignment angle α in the `VELOROOT` framework) is not well determined by the alignment procedure. This angle is therefore set manually such that the detector is centered around the x axis in its local frame. For this purpose, the signal amplitude is determined as a function of $\phi = \tan^{-1}(y/x)$ as shown in figure 4. For those telescope tracks which do not pass through the SCTA detector, the signal on the strip at the corresponding r position is around 0. The edge of the SCTA detector in ϕ is clearly visible. With the available statistics, the precision of this method is limited to $\mathcal{O}(1^\circ)$.[2] For the subsequent analysis, tracks that pass the SCTA detector

[1] "Residual" is defined as radial distance between weighted cluster position and extrapolated track.

[2] Tracks that pass through the boundary between the two inner regions of an r detector lead to a signal

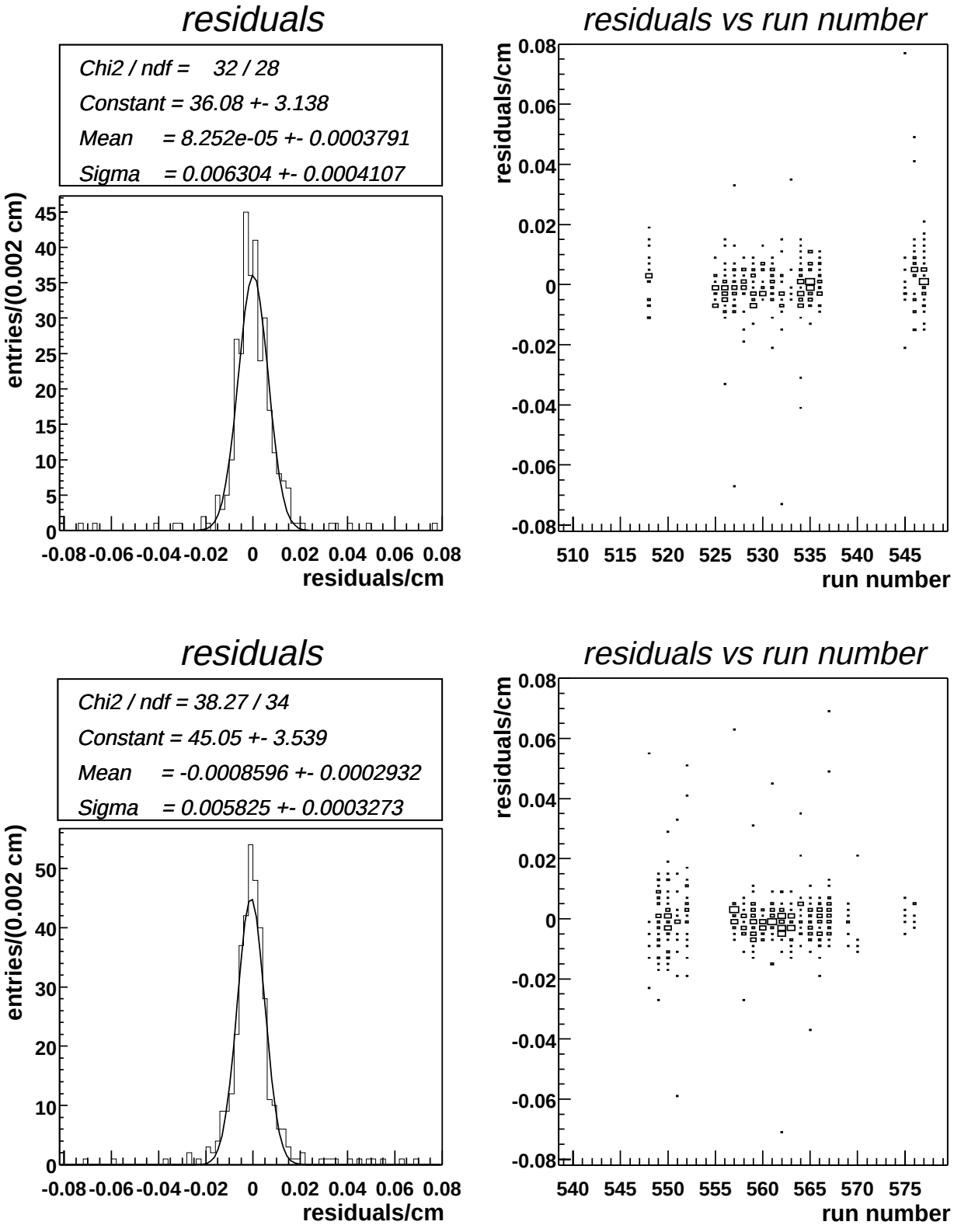

Figure 3: The residuals obtained when performing the alignment separately for two samples of runs.

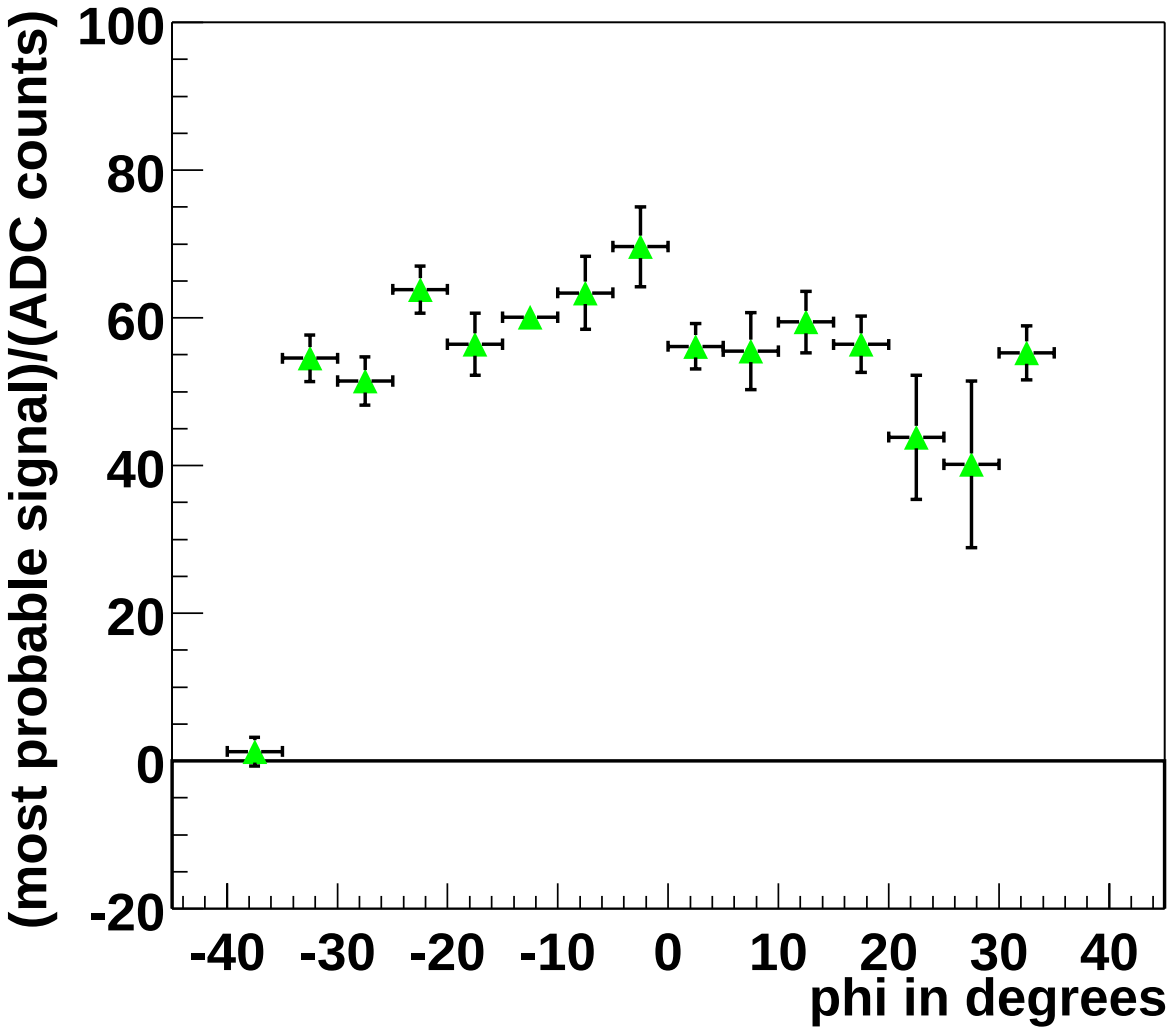

Figure 4: The most probable signal on the SCTA detector is shown as a function of the local ϕ position on the SCTA detector. The signal on the 8 r strips around the extrapolated track position in r is summed. The local ϕ coordinate is determined from the track extrapolation and the alignment constants describing the SCTA detector. For this plot, the alignment angle α has been set manually to zero degrees.

plane outside the active area are not considered.

In the subsequent analysis, the charge signal from the 8 r strips around the extrapolated track position is summed. This corresponds to a 4σ window, assuming identical strip pitches in the three telescope r detectors and the SCTA detector. As a cross-check, the analysis has been repeated with the signal from only 6 strips summed (3σ window), with consistent final results.

4.3 Checks of the Timing Information

For the analysis of the pulse shape, accurate timing information is essential. For most runs in the test beam data, a shift of 594 ns is observed between the TDC timing signal from the scintillators and the readout time t_0 at which the largest signal is seen. In the following, "readout time" is always quoted as the difference between SCTA readout time and scintillator time, corrected for this offset such that the largest signals occur at readout times around zero.

In the Autumn'99 test beam data, two different classes of runs have been found:

- The timing information for runs 526 through 606 has to be shifted by 594 ns as described above such that the highest signals are observed at time "zero".
- For runs 512 through 523, an additional shift of 55 ns is necessary, as shown in figure 5.

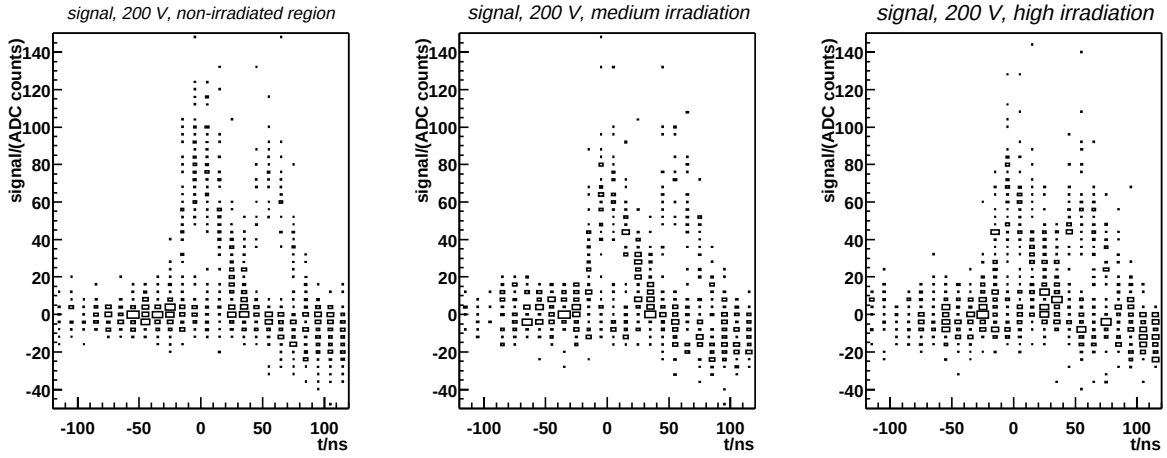

Figure 5: For these plots of the signal on the SCTA detector vs readout time, all runs have been corrected only for the default shift of 594 ns. The contribution from runs 512 through 523, which is offset by 55 ns, is clearly visible.

4.4 Irradiation Profile of the SCTA Detector

The SCTA detector was irradiated on August 27/28, 1999 at the CERN PS with a dose of up to $3.43 \cdot 10^{14}/\mathrm{cm}^2$ 24 GeV protons in the inner (small radius) regions of the detector. The beam was in the plane of the detector such that it gave rise to a highly irradiated band at

on the strips on either side of the boundary and could provide a much more accurate determination of α. An analysis exploiting this feature has been performed [6]. For the study presented in this note, an uncertainty in α of a few degrees is not a limitation.

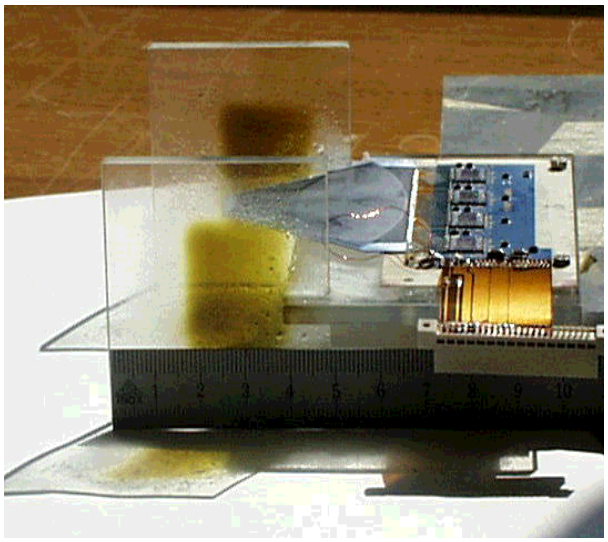

Figure 6: The SCTA detector and hybrid with the mechanical support used during irradiation. The PS beam passed through the setup in the detector plane leaving an irradiated band at small radii on the detector. The beam position is indicated by the brown spots on the plexiglass frame.

small x, independent of the y coordinate of the detector. A picture of the irradiation setup is shown in figure 6. The dose at the point of maximum fluence was measured with a piece of aluminium foil whose mass and activity were measured after the irradiation. This yields the peak value of $3.43 \cdot 10^{14}/\mathrm{cm}^2$ protons [7]. However, the irradiation profile of the detector was not monitored and has to be deduced from later measurements of the beam profile with an irradiated aluminium foil.

A second measurement on November 2/3, 1999 was performed with the same absolute fluence as for the irradiation of the SCTA detector itself. However, only two sets of points in the x direction, which matters for the irradiation profile on the SCTA detector, were measured. The shape of the profile in x is therefore taken from a third measurement of the CERN PS beam profile from April 17th 2000 [8]. Although the absolute fluence of this third measurement is not the same, it can be calibrated with the first measurement and cross-checked with the detailed beam profile in y from the second one.

The results of all measurements are shown in figure 7, where one overall scale factor and arbitrary shifts along x and y are introduced for the measurement from April 2000. The results are in reasonable agreement with each other.

An uncertainty of 0.1 cm is assumed on the position of the centre of the beam in the local frame of the SCTA detector. This dominates over the additional uncertainty of 10% which is assumed as systematic error on the normalisation from the aluminium foil measurements. The irradiation profile of the SCTA detector can then be parameterised as

$$(3.43 \pm 0.34)\ 10^{14}/\mathrm{cm}^2 \cdot \exp\left[-\frac{1}{2}\left(\frac{x - (1.37 \pm 0.10)\,\mathrm{cm}}{0.51\,\mathrm{cm}}\right)^2\right] , \qquad (6)$$

where the central values correspond to the curve in figure 7.

The irradiation of the detector took 12 hours [7]. No detailed information on the annealing history is available for the detector; probably it is over-annealed. For the analysis presented

here, the level of knowledge of the irradiation profile is sufficient to establish the pulse shape of the SCTA chip at different irradiation levels. In the irradiation of detectors for subsequent beam tests, more attention was paid to the irradiation dose, profile, and annealing history.

In figure 8, the expected hit points on the SCTA detector as determined from the extrapolated track positions are shown. The wedge shape of the detector can be clearly seen, together with those regions where the r strips are read out. For the following analysis, the SCTA detector is divided into three regions:

non-irradiated	$3.0\,\mathrm{cm} < x$	$\mathrm{dose} < \left(0.04^{+0.03}_{-0.02}\right) \cdot 10^{14}/\mathrm{cm}^2$
medium irradiation	$2.0\,\mathrm{cm} < x < 2.3\,\mathrm{cm}$	$\left(0.9^{+0.3}_{-0.3}\right) \cdot 10^{14}/\mathrm{cm}^2 < \mathrm{dose} < \left(1.9^{+0.4}_{-0.4}\right) \cdot 10^{14}/\mathrm{cm}^2$
high irradiation	$x < 2.0\,\mathrm{cm}$	$\left(1.9^{+0.4}_{-0.4}\right) \cdot 10^{14}/\mathrm{cm}^2 < \mathrm{dose}$

4.5 Dependence of the Maximum Signal on the Irradiation

In figure 9, the charge signal on the 8 strips around the extrapolated track positions shown in figure 8 is given as a function of readout time, separately for the different bias voltages and for non-irradiated and irradiated detector parts. The time dependence of the signal is clearly visible. The signal spectra for times $-10\,\mathrm{ns} < t < 10\,\mathrm{ns}$ around the central peak are shown in figure 10.

These spectra show clearly a Landau shape, but also have entries around zero charge[3]. They are fitted with a Landau (for the signal) plus a Gaussian centered around zero (describing the noise). For a small number of runs[4], the noise contribution has been found to be very large; these runs are excluded from the analysis.

The most probable values for the Landau distributions as determined in the fit are given in table 2 and shown in figure 11. Here, the irradiated region is further subdivided as stated in the table. While for the non-irradiated area, the signal does not change significantly for voltages between 100 V and 200 V, a strong dependence is observed for the irradiated region.

4.6 Determination of the Pulse Shape

The most probable value of the charge signal is then determined as a function of the readout time in bins of 10 ns width. A fit is performed in a region around the mean of the charge signal in each bin, using a Landau shape with positive (negative) tail if the mean is greater than +10 ADC counts (smaller than −10 ADC counts), and a Gaussian shape otherwise. Although in general, the mean differs from the most probable value because of the Landau tail and because of some noise around zero signal, it provides a first estimate of the most probable value, and the fit converges to the most probable signal. The function is fitted to a region whose width is set to 20 ADC counts + 0.2 · (mean signal), which accounts for the fact that the signal distribution becomes wider for larger signals.

[3]With the present setup, the source of the entries around zero charge cannot be established. It could be due to genuine detector inefficiency, or to events where the particle the scintillators triggered on missed the silicon detectors, but a track from a previous particle is reconstructed in the telescope detectors that are equipped with slow VA2 electronics. The extrapolated track positions for these events to not cluster in particular areas on the detector. This question will be resolved with data taken in a beam test in Summer 2000 where a telescope station with fast electronics had been added so that these two sources can be separated.

[4]These are runs 518, 525, 537, 545, 557, 566, and 567.

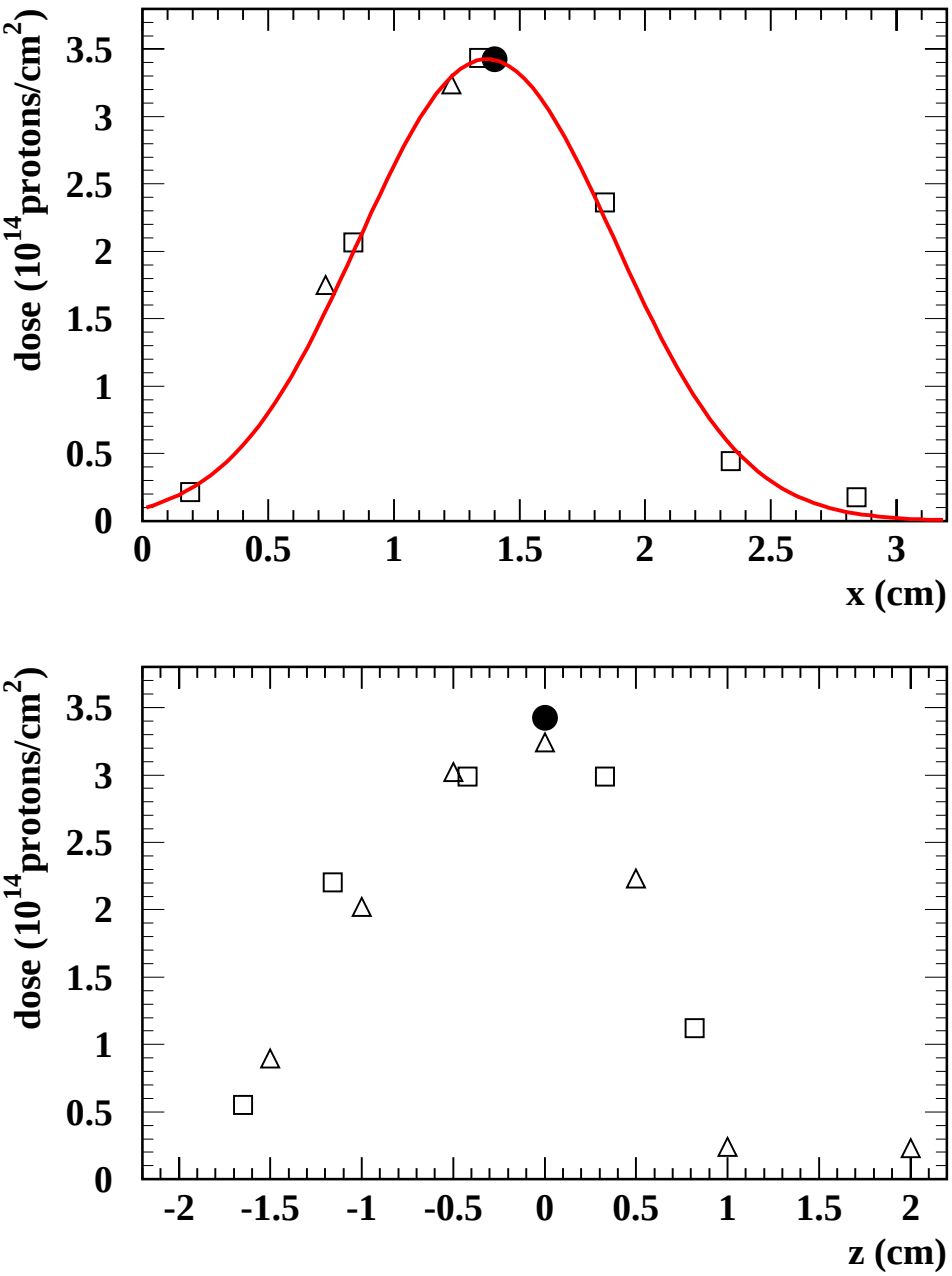

Figure 7: The measurements of the horizontal (upper plot) and vertical (lower plot) profiles of the CERN PS beam. The horizontal axis on the upper plot denotes the local x coordinate on the detector, while the horizontal axis on the lower plot corresponds to the coordinate perpendicular to the detector plane, with the detector located at $z = 0$ (the CERN PS beam passed parallel to the detector plane). The dark circles indicate the measurement performed at the time of the irradiation itself. The open triangles show the measurements taken in November 2/3, 1999, and the open squares indicate those from April 17th 2000. The irradiation of the SCTA detector varies with the horizontal beam profile, as the detector was placed at the maximum of the vertical beam profile during the irradiation. The measurements from April 17th have been scaled such that the maximum values in the upper plot agree. The same scaling factor is applied in the lower plot.

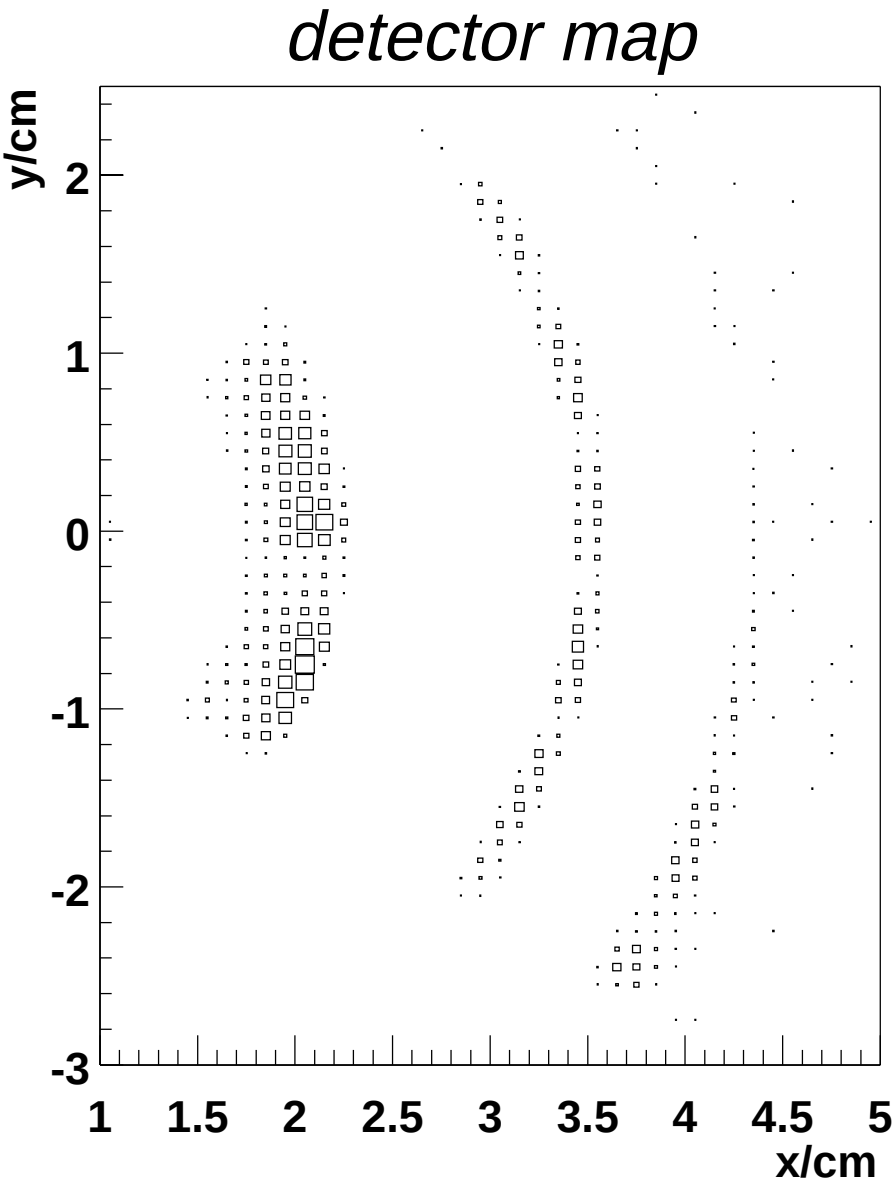

Figure 8: The distribution of points where particles traversed the active areas of the SCTA detector. The symbols x and y denote the local coordinates on the detector.

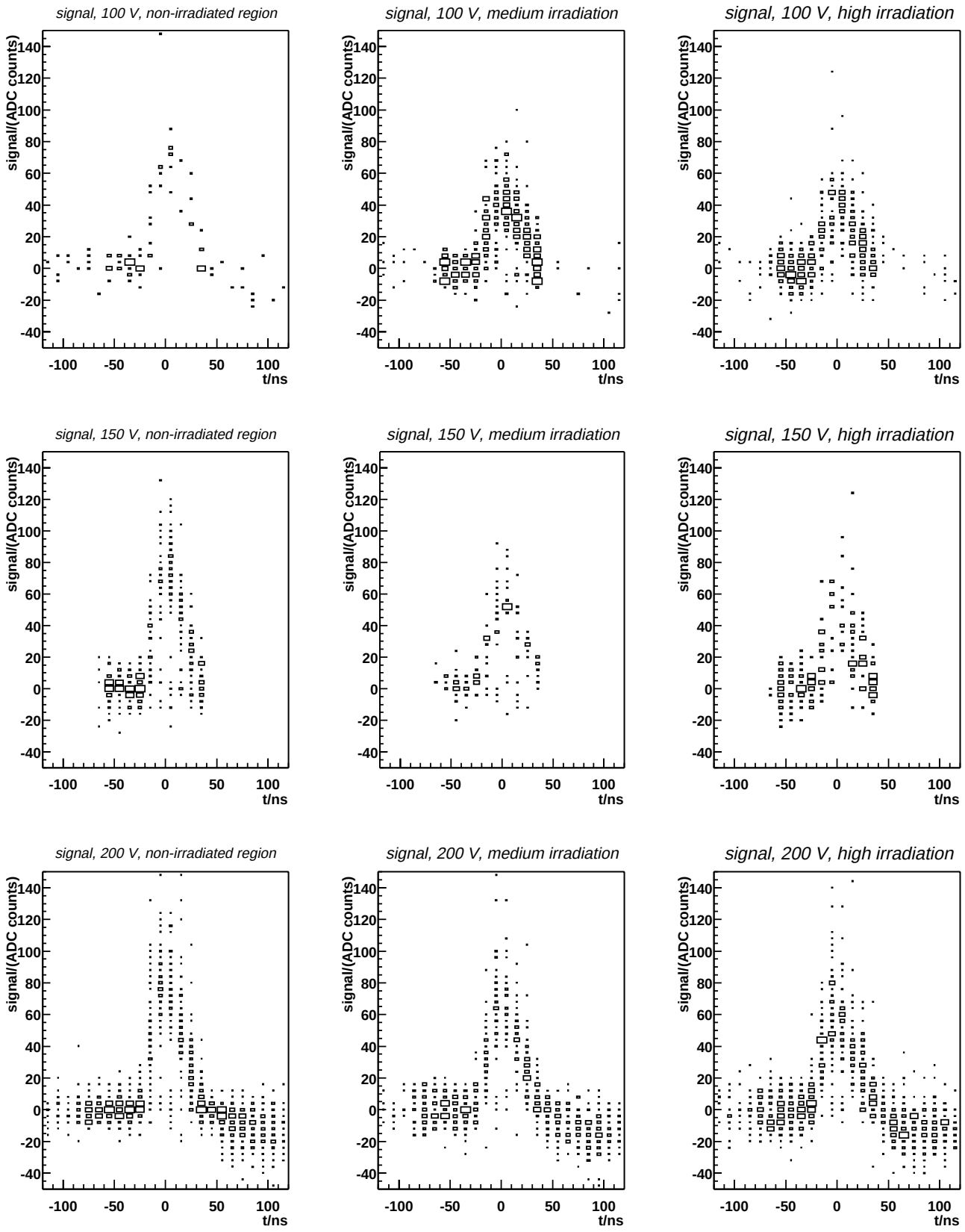

Figure 9: The signals measured as a function of readout time for three different bias voltages are shown separately for the non-irradiated and irradiated regions of the detector.

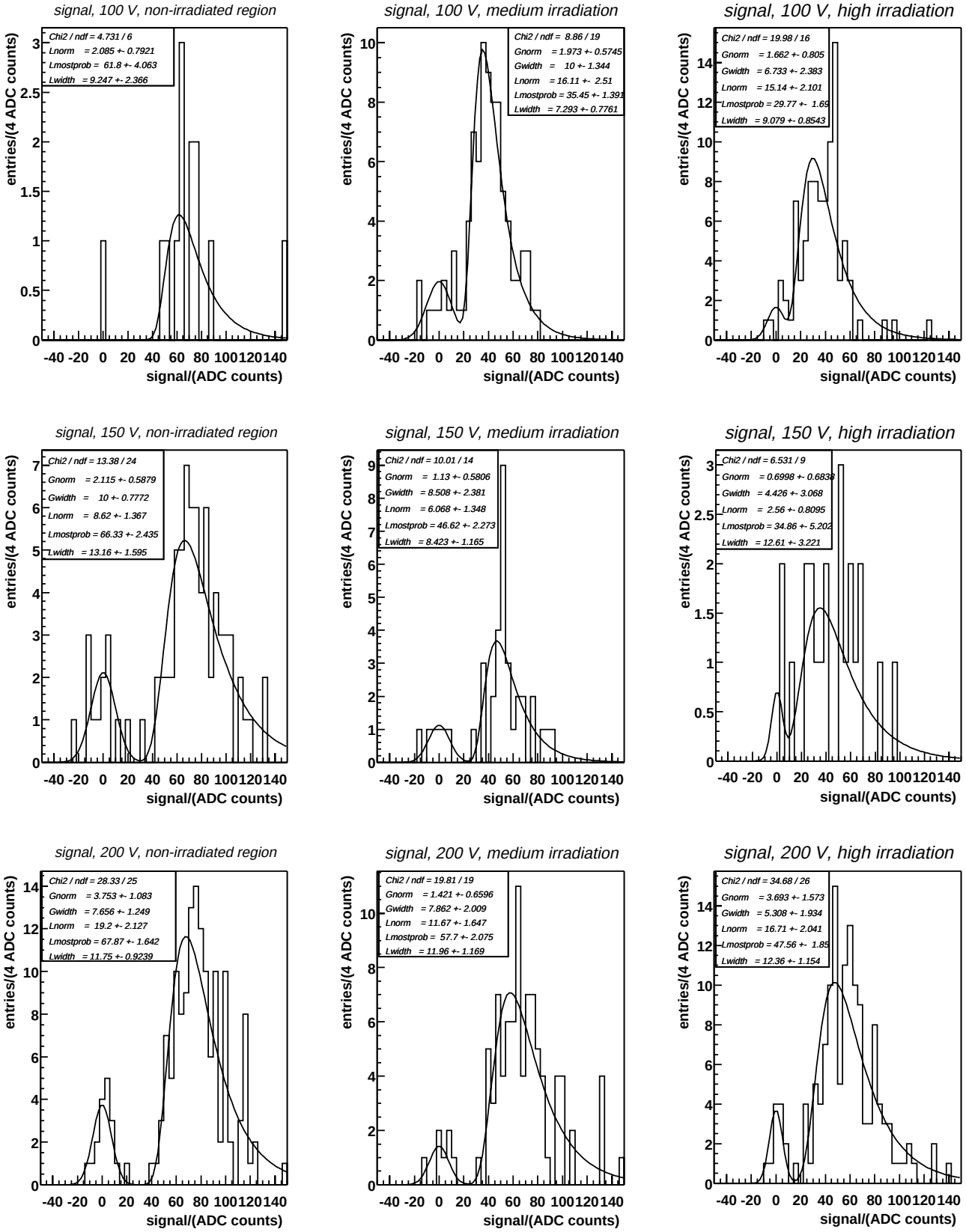

Figure 10: The signals at readout times within $-10\,\text{ns} < t < +10\,\text{ns}$ of the peak for the three different bias voltages and for the non-irradiated and irradiated regions of the detector. In each distribution, the signal Landau can be seen clearly, together with some noise which can be parameterised by a Gaussian centered around zero.

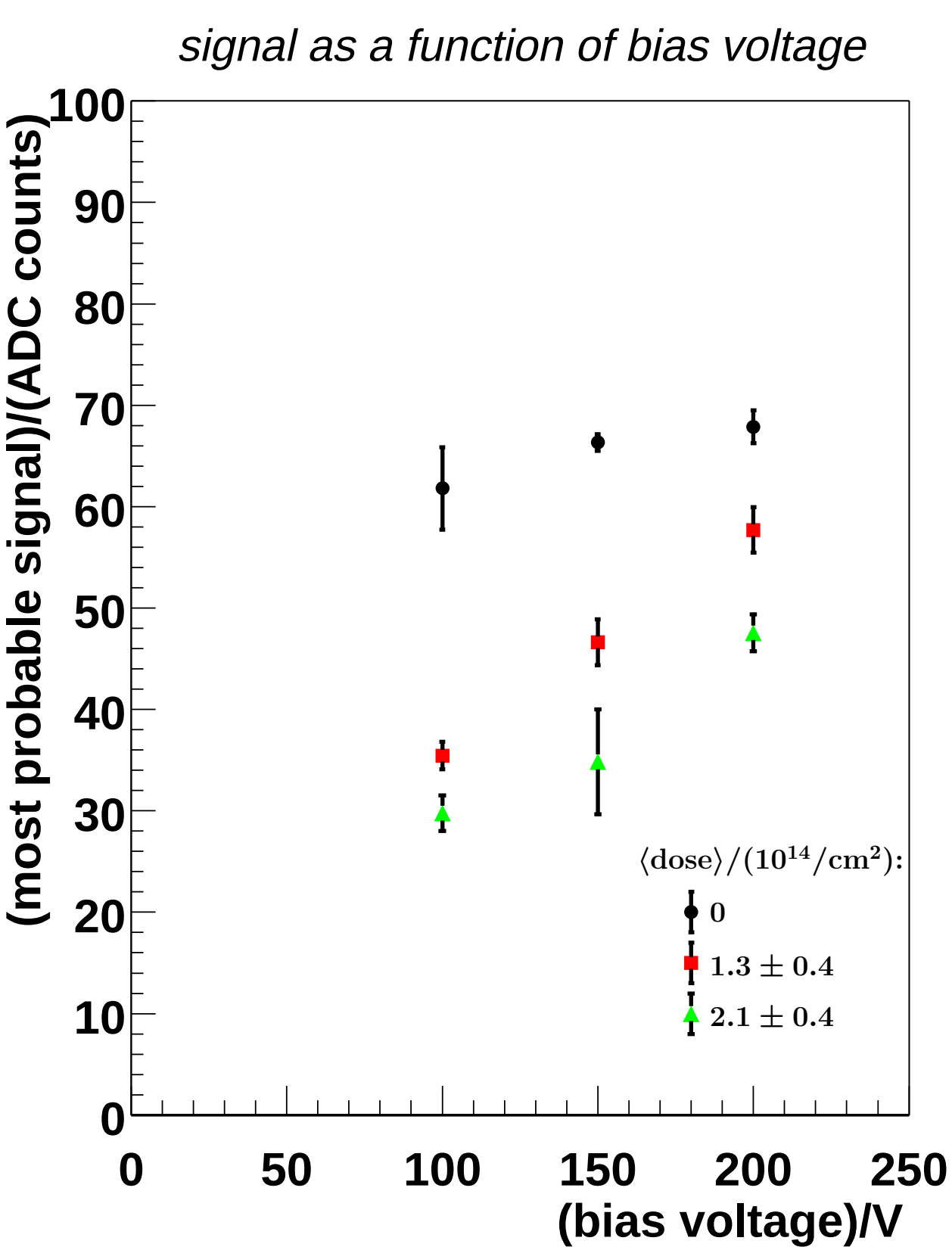

Figure 11: The most probable values of the signal Landaus are shown as a function of the bias voltages for different irradiation levels of the detector.

bias voltage	region on the detector	average dose ($10^{14}/\mathrm{cm}^2$)	signal (ADC counts)
100 V	$x < 2.0\,\mathrm{cm}$	0	61.8 ± 4.1 (*)
	$2.0\,\mathrm{cm} < x < 2.3\,\mathrm{cm}$	$1.25^{+0.38}_{-0.35}$	35.5 ± 1.4
	$3.0\,\mathrm{cm} < x$	$2.11^{+0.39}_{-0.40}$	29.8 ± 1.7
150 V	$x < 2.0\,\mathrm{cm}$	0	66.3 ± 2.4
	$2.0\,\mathrm{cm} < x < 2.3\,\mathrm{cm}$	$1.29^{+0.40}_{-0.34}$	46.6 ± 2.3
	$3.0\,\mathrm{cm} < x$	$2.13^{+0.43}_{-0.44}$	34.9 ± 5.2
200 V	$x < 2.0\,\mathrm{cm}$	0	67.9 ± 1.6
	$2.0\,\mathrm{cm} < x < 2.3\,\mathrm{cm}$	$1.28^{+0.39}_{-0.35}$	57.7 ± 2.1
	$3.0\,\mathrm{cm} < x$	$2.07^{+0.42}_{-0.43}$	47.6 ± 1.8

Table 2: The most probable values of the signal Landau distributions, determined for different bias voltages and doses as indicated in the table. The most probable values have been determined from a fit of a Gaussian+Landau to the signal within readout times of $-10\,\mathrm{ns} < t < +10\,\mathrm{ns}$. An exception is the value indicated by (*), where only a Landau has been fitted because of the limited statistics.

5 Results

5.1 Measurement of the SCTA Pulse Shape

The resulting distributions of most probable values as a function of readout time are shown in figure 12. They have been fitted with the parameterisation of the pulse shape that has been discussed in section 2.

It is observed that this parameterisation describes the signal shapes very well. The parameters of the function are:

parameter		meaning
height	(fitted)	the overall normalisation (in ADC counts) of the curve;
pole a, pole b	(fitted)	the two poles (in GHz) describing the SCTA response;
t_{rise}, t_{plateau}, and t_{fall}	(fixed)	the parameters (in ns) describing the input signal to the SCTA chip, see figure 1;
t_{maxpulse}	(fitted)	a parameter (in ns) providing the necessary offset along the t axis of the fitted function.

It has been found that the pulse shape is very insensitive to the parameter t_{plateau}. On the other hand, t_{rise} and t_{fall} are highly correlated with the values of the poles a and b of the SCTA chip. Since the main purpose of the analysis is to determine the overspill fraction as a function of readout time, the parameters t_{rise}, t_{plateau}, and t_{fall} are fixed to 1 ns, 3 ns, and 1 ns, respectively. This results in a good description of the observed signal, and the fitted functions are used in the determination of the overspill fraction, as discussed in the following section.

5.2 Determination of the Optimal Readout Time for LHCb

At LHC, bunch crossings will occur every 25 ns. It is therefore crucial that the signals due to the particles from one bunch crossing decay fast enough to ensure that they do not mimick tracks in the subsequent event. It has been estimated that the overspill fraction, defined as the

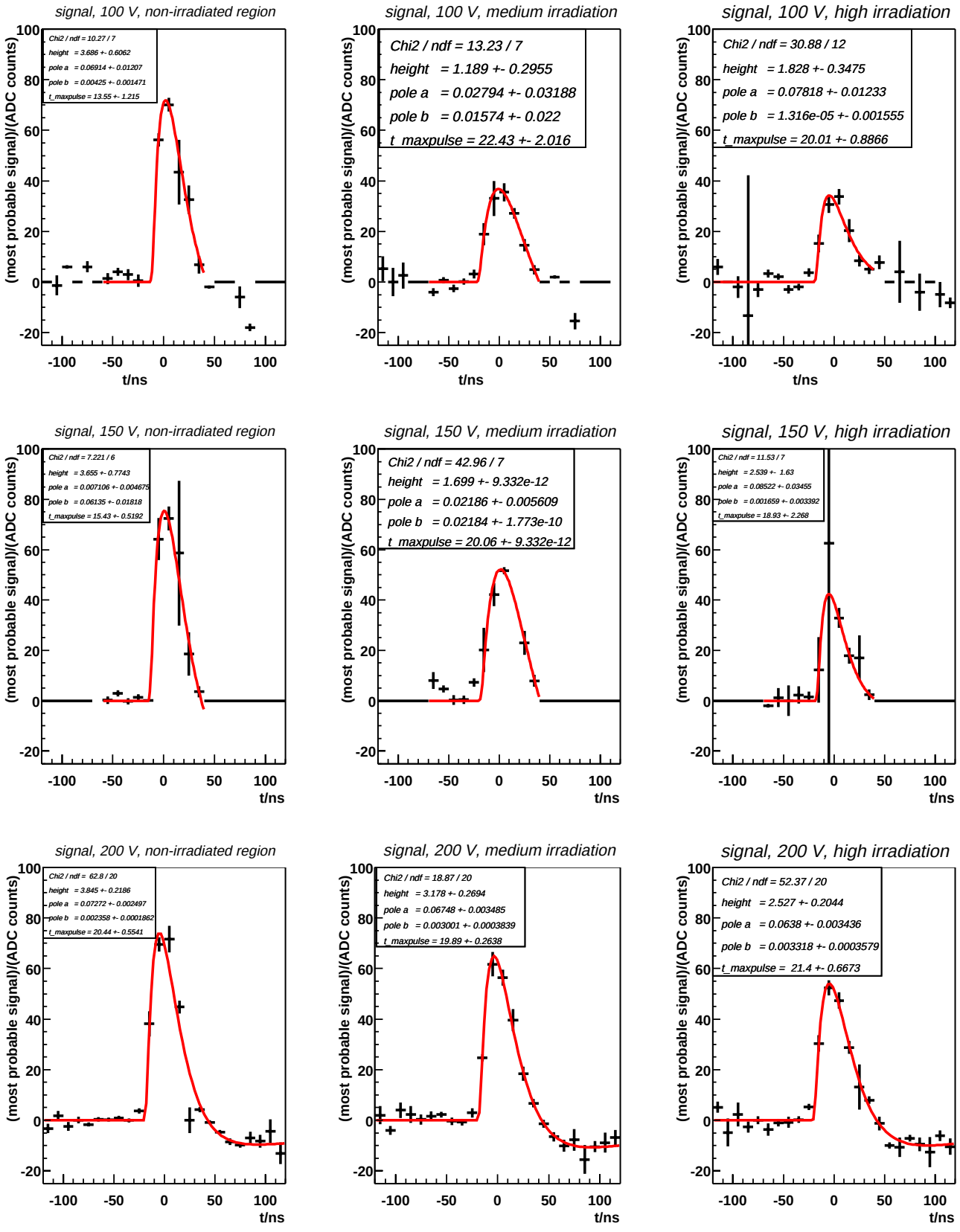

Figure 12: The most probable signal values as a function of the readout time for the three different bias voltages, separately for the non-irradiated and irradiated regions of the detector. The results of fits to the distributions are superimposed.

fraction of the signal amplitude that remains after 25 ns, should not be greater than 30% [9]. The readout time of the SCTA chip should be tuned such that the overspill fraction remains below the critical value while the signal amplitude is as large as possible.

The time dependence of the SCTA output signal is extracted from the fits to the data taken at 200 V bias voltage where the largest window in readout times is covered. The analysis is performed separately for the non-irradiated, medium irradiated, and highly irradiated regions on the detector; the latter two regions are read out by the same SCTA chip. The results are shown in figure 13:

- For each region, the wide solid curve indicates the fraction of the maximum possible signal as a function of the SCTA readout time. This curve corresponds to the fitted function shown in figure 12. The dependence of the signal on the readout time is the same for the two irradiated regions. The pulse shape is slightly narrower for the SCTA chip reading out the non-irradiated region. From point of view of this signal alone, the optimal readout time would be around $t \sim -1$ ns for the non-irradiated and $t \sim -4$ ns for the irradiated regions.
- The dashed curves show the overspill fractions seen from the signals in events at 25 ns, 50 ns, and 75 ns before the event in consideration, as a function of the SCTA readout time. The overspill fraction at a given readout time is not normalised to the maximum possible signal (100% in the plots) but to the signal that is actually obtained at the given readout time, which is in general less than 100% according to the wide solid curve. This definition is sensible because the analysis presented here addresses the possibility to distinguish between clusters from different beam crossings as a function of readout time. The answer to this question depends on the difference between measured signal heights, irrespective of the maximum possible signal that could be obtained at some time t_0 at which the information is not actually read out. The vertical scale in the plots has thus two different meanings: Signal normalised to maximum possible signal (solid curve) and overspill normalised to signal at the same readout time (dashed and dash-dotted curves).

  The condition that this overspill fraction be less than 30% constrains the available readout times, for instance in the irradiated regions readout of the chip at $t = -4$ ns would result in an overspill fraction of about 40%.
- In addition, the dash-dotted lines indicate the "underspill" fraction from signals in the beam crossing at 25 ns *after* readout: If the readout time is set too late, events from the *subsequent* beam crossing may spoil the event in question. Again, the underspill fraction at each readout time is normalised to the available signal at that particular time.

  Because of the sharp rise of the SCTA signal, the 30% maximum allowed underspill do not severely constrain the allowed readout times: Such late readout times are anyway not advantageous in terms of the signal amplitude itself.

In both the non-irradiated and irradiated regions, it is possible to obtain a working point where less than 30% overspill is seen. In addition, the signal loss relative to the readout time with the largest signal can be kept small if the readout time is adjusted to within a few nanoseconds to minimise this loss. The limitations on the possible working point are summarised in table 3.

In the analysis presented here, only the seperation between the signal from different beam crossings has been considered. The separation between signal clusters and noise has not been addressed. In principle, the minimum allowed cluster signal to noise ratio also constrains the possible readout times. However, since it has been shown that the signal loss after tuning of

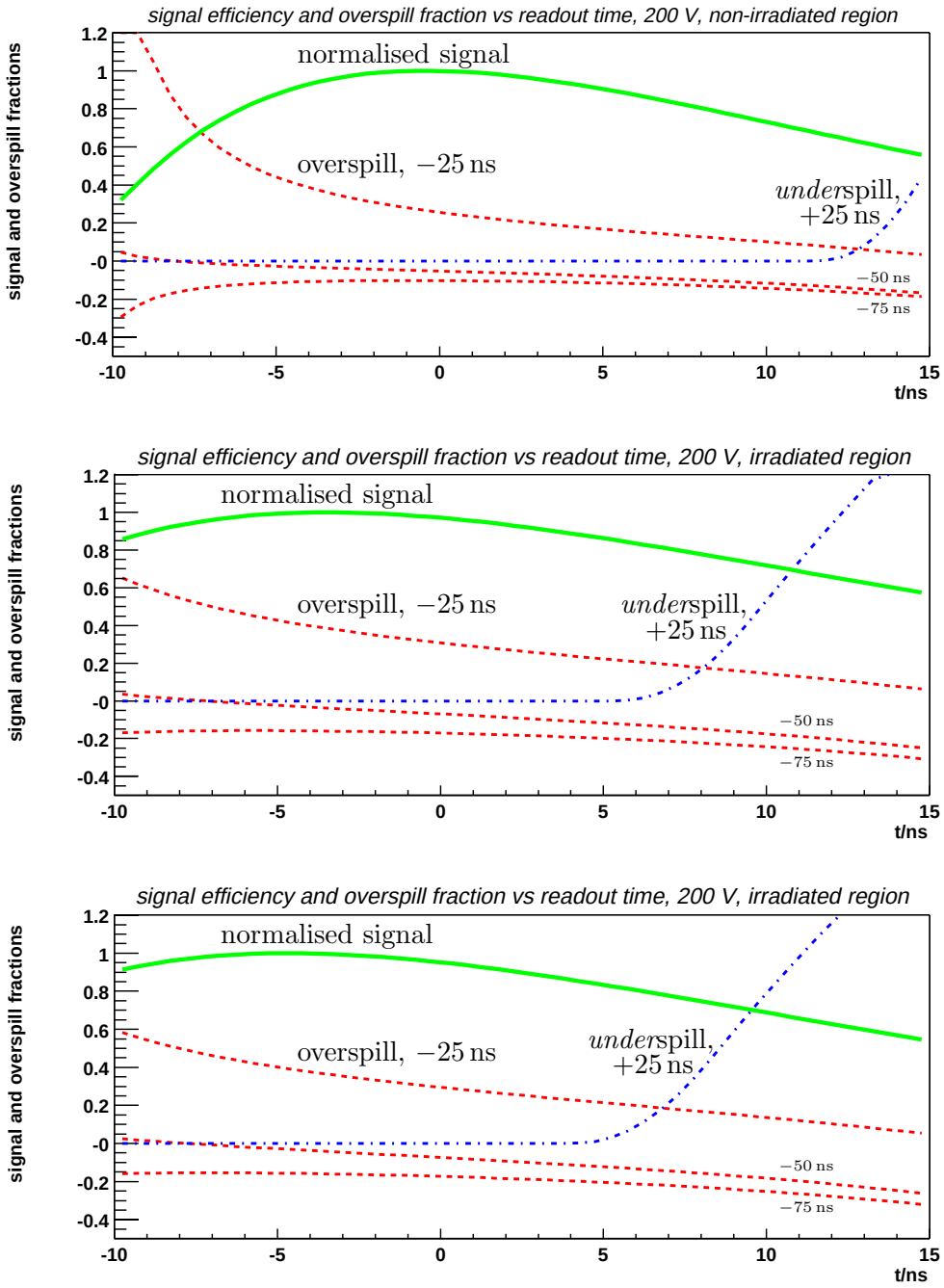

Figure 13: Analysis of the available signal and the overspill fraction vs. SCTA readout time for the non-irradiated (upper histogram), medium irradiated (middle histogram), and highly irradiated (lower histogram) areas of the detector, read out with 200 V bias voltage. In each plot, the signal fraction (normalised to the maximum possible signal) as a function of readout time is given by the wide solid curve. The overspill fractions from events at −25 ns, −50 ns, and −75 ns as a function of readout time, normalised to the signal at the same readout time, are given by the dashed lines. Similarly, the underspill fraction from the next event is shown by the dash-dotted line.

200 V, non-irradiated area $\langle \text{dose} \rangle = 0$	
readout time	available signal
$t_{\min} = -1.3\,\text{ns}$	100%
$t_{\max} = 14.2\,\text{ns}$	58%

200 V, area with medium irradiation $\langle \text{dose} \rangle = \left(1.28^{+0.39}_{-0.35}\right) \cdot 10^{14}/\text{cm}^2$	
readout time	signal fraction
$t_{\min} = 0.4\,\text{ns}$	97%
$t_{\max} = 8.9\,\text{ns}$	75%

200 V, area with high irradiation $\langle \text{dose} \rangle = \left(2.07^{+0.42}_{-0.43}\right) \cdot 10^{14}/\text{cm}^2$	
readout time	signal fraction
$t_{\min} = 0.3\,\text{ns}$	94%
$t_{\max} = 7.5\,\text{ns}$	77%

Table 3: The range of readout times for which the overspill fraction is smaller than 30% is given. The overspill fraction is defined as the fraction of the signal at the readout time in question that is present 25 ns prior or after the readout time. In addition, the signal fraction at the limits of the allowed time window relative to the highest possible signal is also indicated.

the overspill fraction is small, this question is not an important issue[5].

6 Conclusions

Data from the beam test in Autumn 1999 have been analysed to determine the pulse shape of the SCTA readout chip for the LHCb VELO. It has been found that the pulse shape is in excellent agreement with expectations. The shape of the SCTA output signal is such that the VELO is not adversely affected by the overspill from previous bunch crossings if an appropriate readout time is chosen. This choice of readout time may lead to a signal reduction of a few per cent. The pulse shape of the SCTA chip is essentially independent of the irradiation the silicon detector received, up to at least the equivalent of about one year's operation within the LHCb experiment.

References

[1] W. Dąbrowski et al., *A Prototype Chip for Binary Readout of Silicon Strip Detectors,* Nucl. Instrum. Meth. **A 421** (1999) 303;
F. Anghinolfi et al., *Development of Front End Electronics for Silicon Strip Detectors Using the DMILL BiCMOS rad-hard Process,* in: Proceedings of the 2nd Workshop on

[5] Remaining overspill clusters will of course be difficult to distinguish from noise, but in this case this is a feature, not a bug...

Electronics for LHC Experiments, Balatonfured, Hungary (1996) 483;
F. Anghinolfi *et al.*, *SCTA – A rad-hard BiCMOS analogue readout ASIC for the ATLAS semiconductor tracker,* IEEE Trans. Nucl. Sci. **44** (1997) 298;
C. Posch, Dissertation, *Analog Readout for the ATLAS Semiconductor Tracker*, Vienna University of Technology, Institute for Applied Electronics and Quantum Electronics, Gußhausstraße 25-29, A-1040 Vienna, Austria.

[2] E. Fairstein, *Bipolar pulse shaping revisited,* IEEE Transactions on Nuclear Science (USA), Vol. 44, No. 3, Pt. 1, pp. 424-428 (June 1997 / NSS'96 Anaheim, CA, USA).

[3] S. Saladino, *Study of vertex silicon detectors for LHC experiments*, thesis (CERN-OPEN-99-374), 3 December 1999.

[4] C. Parkes, *Detector Geometry – Vertex Locator Test-Beam Software Description*, LHCb 2000-096 (26. 10. 2000);
C. Parkes, *Track Fitting – Vertex Locator Test-Beam Software Description*, to be published as an LHCb note.

[5] I. Tomalin, *Alignment of the 1998 VELO test beam data,* LHCb 99-032, VELO, internal note (27. 8. 1999).

[6] H. Smith, *Search for Pixel Clusters in the VELO Silicon Strip Detector*, LHCb 2000-25, VELO, internal note (18. 8. 2000).

[7] Information from the irradiation logbook in office `14 R-012` at CERN.

[8] G. Casse, private communication.

[9] P. Koppenburg, *Simulation of the vertex trigger preprocessor: Effects of noise on L1 performance*, LHCb TRIG 99-003 (22. 2. 1999).